Separation Science and Technology
Publication details, including instructions for authors and subscription information:
http://www.informaworld.com/smpp/title~content=t713708471

Modification of Single-walled Carbon Nanotubes for Enhancing Isopropyl Alcohol Vapor Adsorption from Air Streams

Shihchieh Hsu[a]; Chungsying Lu[a]
[a] Department of Environmental Engineering, National ChungHsing University, Taichung, Taiwan

To cite this Article Hsu, Shihchieh and Lu, Chungsying(2007) 'Modification of Single-walled Carbon Nanotubes for Enhancing Isopropyl Alcohol Vapor Adsorption from Air Streams', Separation Science and Technology, 42: 12, 2751 — 2766
To link to this Article: DOI: 10.1080/01496390701515060
URL: http://dx.doi.org/10.1080/01496390701515060

Separation Science and Technology, 42: 2751–2766, 2007

ISSN 0149-6395 print/1520-5754 online
DOI: 10.1080/01496390701515060

Modification of Single-walled Carbon Nanotubes for Enhancing Isopropyl Alcohol Vapor Adsorption from Air Streams

Shihchieh Hsu and Chungsying Lu
Department of Environmental Engineering, National ChungHsing University, Taichung, Taiwan

Abstract: Single-walled carbon nanotubes (SWCNTs) were oxidized by HCl, HNO_3 and NaClO solutions and were selected as adsorbents to study their characterizations and adsorption properties of isopropyl alcohol (IPA) vapor from air streams. The physicochemical properties of SWCNTs were greatly changed after oxidation by HNO_3 and NaClO solutions. These modifications include the increase in surface functional groups and surface basic sites, which enhance the chemisorption capacity of IPA, and the decrease in pore size and the increase in surface area of micropores, which improve the physisorption capacity of IPA. The maximum IPA adsorption capacities of SWCNTs, SWCNTs(HCl), SWCNTs(HNO_3) and SWCNTs(NaClO) calculated by Langmuir model are 63.48, 54.34, 72.99, and 103.56 mg/g, respectively. The SWCNTs(NaClO) show the best performance of IPA removal and their adsorption mechanism appears mainly attributable to physical force with a relatively low influent IPA concentration but appears attributable to both physical and chemical forces with a relatively high influent IPA concentration.

Keywords: Single-walled carbon nanotubes, chemical modification, adsorption, isopropyl alcohol vapor

INTRODUCTION

Carbon nanotubes (CNTs) are unique and one-dimensional macromolecules that have outstanding thermal and chemical stability (1). These nanomaterials

Received 5 February 2007, Accepted 19 March 2007
Address correspondence to Chungsying Lu, Department of Environmental Engineering, National ChungHsing University, 250 Kuo Kuang Road, Taichung 402, Taiwan. Fax: +886-4-2286-2587; E-mail: clu@nchu.edu.tw

have been proven to possess good potential as superior adsorbents for removing many kinds of organic and inorganic pollutants in air streams (2, 3) or from aqueous environments (4–10). The large adsorption capacity of CNTs is mainly attributable to their pore structure, surface area, and the existence of a wide spectrum of surface functional groups. A modification of CNTs with specific physicochemical properties can be achieved by chemical or thermal treatments to make CNTs that possess optimum performance for particular purposes. Therefore, a test on the modification method of CNTs is needed for employing the most efficient CNTs in order to meet the growing demand for cleaner air and water.

Isopropyl alcohol (IPA) is a widely used volatile organic compound (VOC). In addition to its use as a solvent, it is frequently encountered in the manufacture of opto-electronic apparatus and semi-conductors that are the most important industries in Taiwan. Due to the lack of a proper air pollution control device, many IPA vapors are released into the atmosphere during the manufacturing process every year. Loss of these irritative and carcinogenic substances (11) to ambient air may lead to an adverse effect on the air quality and thus endanger public health and welfare.

In this article, single-walled CNTs (SWCNTs) were oxidized by HCl, HNO_3, and NaClO solutions and were employed as adsorbents to study their characterizations. Adsorption properties of IPA vapor by raw and oxidized SWCNTs were also conducted to determine the optimum chemical modification in IPA treatment.

MATERIALS AND METHODS

Adsorbents

Commercially available SWCNTs with inner diameter of <2 nm (L-SWCNTs, Nanotech Port Co., Shenzhen, China) were selected as adsorbents in this study. The length of CNTs was in the range 5–15μm and the mass ratio of amorphous carbon content in the CNTs was <5 wt%. These data were provided by the manufacturer.

Raw SWCNTs (3 g) were treated by HCl (JT Baker, NJ, USA, 65% purity), HNO_3 (JT Baker, NJ, USA, 68% purity) and 30% NaClO (70 ml of H_2O + 30 ml of 70% purity NaClO) solutions. These chemical agents have been used to oxidize activated carbon for enhancing the removal of environmental pollutants (12). The mixed solution was shaken in an ultrasonic cleaning bath (Model D400H, Delta Instruments Co., USA) for 20 min and was heated at 85°C in a water bath for 3 h to remove metal catalysts (Ni nanoparticles). After cooling to room temperature, the mixture was filtered through a 0.45 μm nylon fiber filter and the solid was washed with deionized water until the pH of the filtrate was 7. The filtered solid was then dried at 210°C for 2 h. The weight loss of SWCNTs after treatment was <4%.

Experimental Set-up

The experimental set-up for IPA adsorption onto SWCNTs is shown in Fig. 1. The adsorption column was made of Pyrex having a length of 20 cm and an internal diameter of 1.5 cm. The adsorption column was filled with 1.0 g SWCNTs (packing height = 4.0 cm) and was placed within a temperature control box (Model CH-502, Chin Hsin, Taipei, Taiwan) to maintain temperature at 25°C.

Compressed air was passed first through a filtration device (LODE STAT compressed air dryer, Model LD-05A, Taipei, Taiwan) to remove moisture, oil, and particulate matter. After filtration, the minor air stream was passed through the first glass bottle containing IPA solution (JT Baker, NJ, USA, 99.9% purity) to produce IPA vapor which was mixed with the major air stream in the second glass bottle. The mixed air was then passed downwards into the adsorption column. The influent IPA concentration and the system flow rate were controlled by regulating the minor air stream rate and the major air stream rate, respectively, using mass flow controllers (Model 247C four channel read-out and model 1179A for mass flow controllers, MKS instrument Inc., MA, USA). The influent and effluent air streams

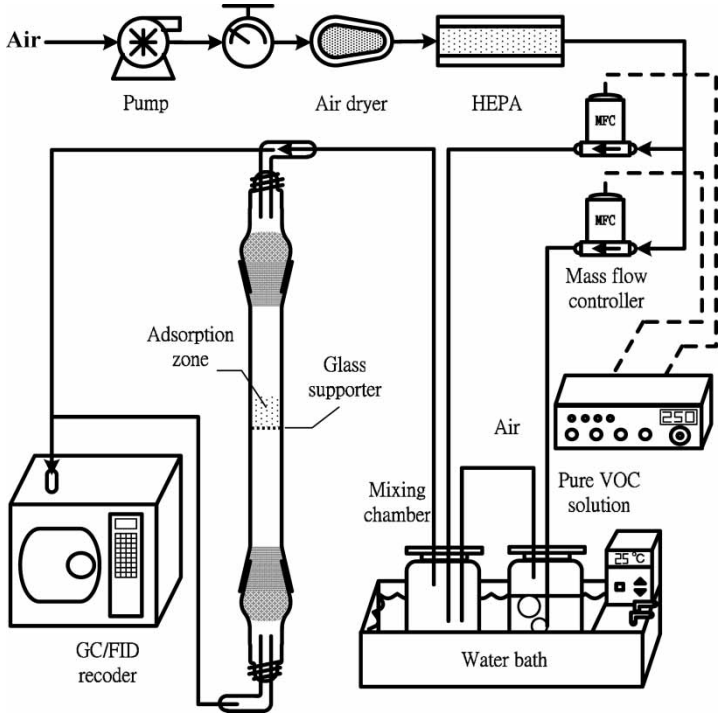

Figure 1. Schematic diagram of the experimental setup.

were flowed into a gas chromatograph (GC) equipped with a flame ionization detector (FID) by an auto sampling system. The variations in the influent IPA concentration were within 5% and the system flow rate was controlled at 0.08 lpm which is equivalent to an empty-bed retention time of 5.3 s.

The amount of IPA adsorbed onto adsorbents (q, mg/g) was calculated as:

$$q = \frac{1}{m}\int_0^t Q \cdot \left(C_{in} - C_{eff}\right)dt \tag{1}$$

where m is the mass of virgin adsorbents (g); t is the contact time (min); Q is the influent flow rate (lpm); and C_{in} and C_{eff} are the influent and effluent IPA concentrations (mg/l), respectively.

Most adsorption processes are a combination of a physical process (physisorption) and a chemical process (chemisorption). The equilibrium IPA capacities of physisorption (q_{ep}, mg/g) and chemisorption (q_{ec}, mg/g) were estimated. As the adsorption reached equilibrium, the IPA adsorption capacity was measured and then the influent air stream was changed to N_2 gas which was controlled at a Q of 0.1 l pm. The outlet of the adsorption column was connected to a vacuum pump and was operated in 65 mm-Hg until the IPA vapor in effluent streams was undetectable. The q_{ec} and q_{ep} were calculated as:

$$q_{ec} = \frac{m_1 - m}{m} \times 1000 \tag{2}$$

$$q_{ep} = q_e - q_{ec} \tag{3}$$

where m_1 is the mass of spent adsorbents after vacuum suction (g); q_{e} is the amount of IPA vapor adsorbed at equilibrium onto adsorbents (mg/g).

Analytical Methods

IPA concentration in the air stream was determined using a GC-FID (Model SRI 8610C, SRI Instruments, CA, USA). A 15 m fused silica capillary column with 0.32 mm inner diameter and 1.0 μm film thickness (Supelco wax, Supelco Inc., PA, USA) was used for IPA analysis. The GC-FID was operated at injection temperature of 150°C, detector temperature of 200°C, and oven temperature of 130°C.

The morphology of adsorbents was analyzed by a high-resolution transmission electron microscope (HR-TEM, Model JEM-2010, JEOL, Tokyo, Japan). The physical properties of adsorbents were determined by N_2 adsorption at 77 K using ASAP 2010 surface area and porosimetry analyzer (Micromertics Inc., Norcross, GA, U.S.A.). N_2 adsorption isotherms were measured at a relative pressure range 0.0001–0.99. The adsorption data were then employed to determine surface area of adsorbents using the Brunauer, Emmett and Teller (BET) equation. The pore size distributions (PSDs) of adsorbents were determined from the N_2 adsorption data using the Barrett, Johner and

Halenda (BJH) equation for mesopores and macropores (1.7 < pore size < 100 nm) and the MP equation for micropores (pore size < 1.7 nm).

The chemical properties of adsorbents were based on the surface functional groups and the surface basic sites. The surface functional groups of adsorbents were detected by a Fourier transform infrared (FTIR) spectrometer (Model FT/IR-200, JASCO Inc., Japan) while the surface basic sites of adsorbents were determined using the Boehm titration method (13). 100 mg of adsorbents were placed in a 100 ml flask containing 50 ml of 0.1 M NaOH solution which was sealed and shaken for 48 h. The solution was then filtered through a 0.45 μm nylon fiber filter and 10 ml of each filtrate was pipetted. The excess of the base was titrated with 0.1 M HCl. The basic site concentration was determined from the amount of HCl reacted with the adsorbents.

The structure information of adsorbents was evaluated by a Raman spectrometer (Model Nanofinder 30 R., Tokyo Instruments Inc., Japan). The carbon content in the adsorbents was determined by a thermogravimetric analyzer (Model TG209 F1 Iris, NETZSCH, Bavaria, Germany)

RESULTS AND DISCUSSION

TEM

Figure 2 exhibits the TEM images of adsorbents. It is evident that the SWCNTs contained an atomic layer structure with an outer diameter of 3–4 nm and with the hollow inner tube diameter of 1.7–2.5 nm. Due to inter-molecular force, the isolated SWCNTs of different size and direction form an aggregated structure. The SWCNTs(NaClO) showed large quantities of nanotubes bundles with the hollow inner tube diameter of ~2.0 nm. A great amount of carbon-containing defects along the surface of SWCNTs(HNO_3) and SWCNTs(NaClO), which can be easily introduced as surface functional groups and thus provide numerous chemical adsorption sites. The TEM image of SWCNTs(HCl) showed more smooth carbon surfaces and less structure defects than those of SWCNTs(HNO_3) and SWCNTs(NaClO).

BET

Figure 3 presents the adsorption and desorption isotherms of N_2 onto adsorbents. It is apparent that all curves display a type IV adsorption isotherm according to the IUPAC classification (14), with a rounded knee at low relative pressures representing a micropore volume in the SWCNTs, a plateau with a sharp slop at high relative pressures accompanied by hysteresis indicating a capillary condensation of N_2 within mesopores. The SWCNTs and SWCNTs(HCl) have a greater adsorption capacity of N_2 than the SWCNTs(HNO_3) and SWCNTs(NaClO), reflecting that a greater amount of porosity in SWCNTs and SWCNTs(HCl) (15).

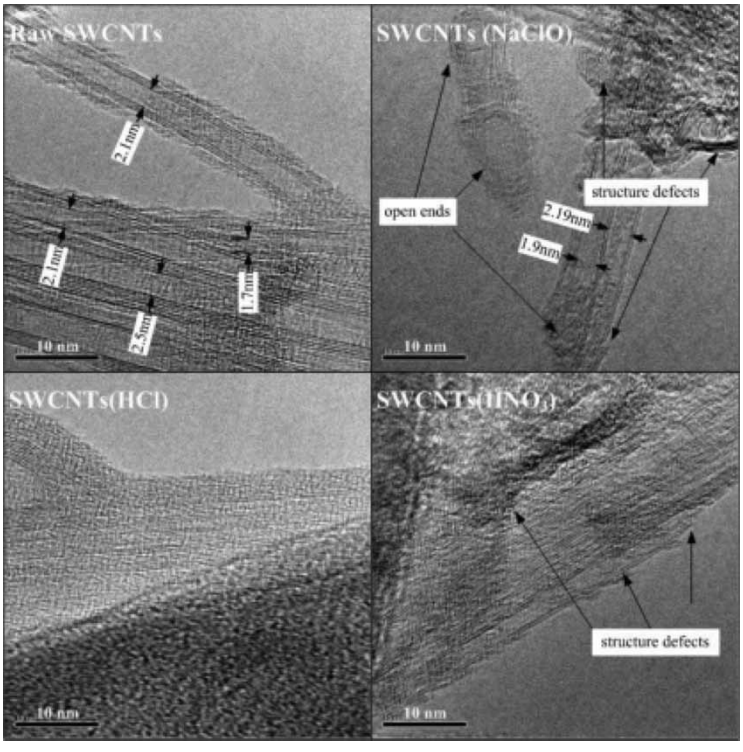

Figure 2. Transmission electron microscopic images of adsorbents.

The PSDs of adsorbents are presented in Fig. 4 and display a bimodal distribution including a fine fraction and a coarse fraction. The pores in the fine fraction are the CNT inner cavities, close to the inner CNT diameter while the pores in the coarse fraction are likely to be contributed by aggregated pores which are formed within the confined space among the isolated SWCNTs. The fine and coarse fractions, respectively, concentrated in the 1-3 and 7–12 nm width range for the SWCNTs and SWCNTs(HCl), and 1-2 and 3–5 nm width range for the SWCNTs(HNO_3) and SWCNTs(NaClO). Both the aggregated pores and the inner cavities of SWCNTs decreased after oxidation by HNO_3 and NaClO solutions.

The physical properties of the adsorbents are given in Table 1. The average pore diameters become smaller, the surface areas of pore size 5–100 nm remarkably decrease, and most pore volumes are of size $\leq$5 nm after the SWCNTs were oxidized by HNO_3 and NaClO solutions. This could be explained from the observations by a scanning electron microscope that the length of SWCNTs became short and the confined space among isolated SWCNTs appeared narrow after oxidation by NaClO solutions (9). Moreover, pore entrance blockage by the formation of functional groups

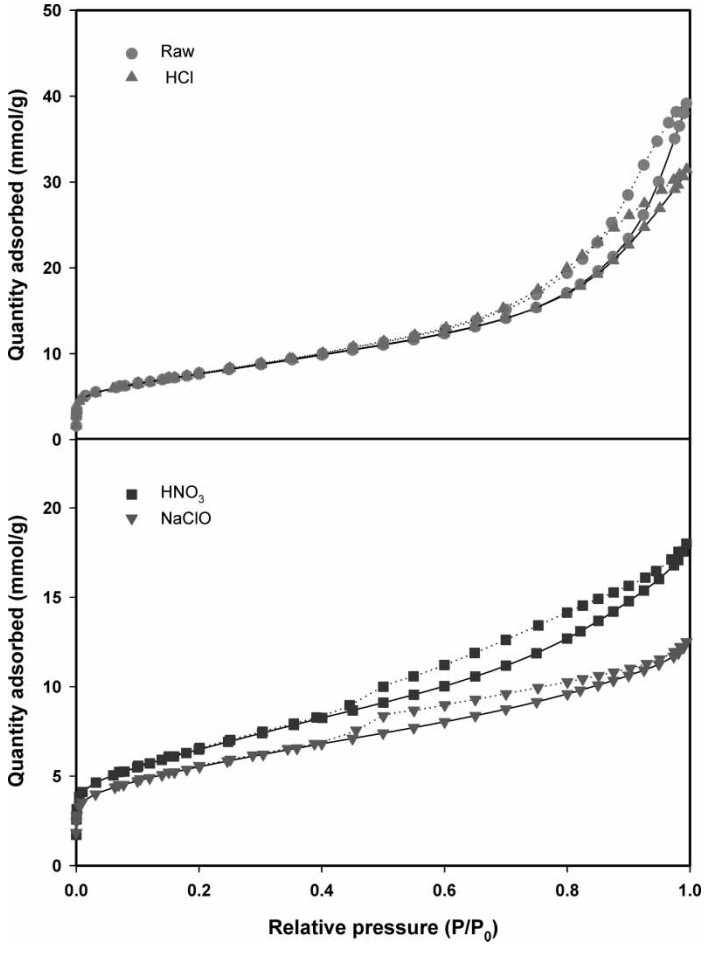

Figure 3. Adsorption (solid line) and desorption (dash line) isotherms of N_2 onto adsorbents.

that are direct products of HNO_3 and NaClO oxidation may also cause the decrease in surface area, pore volume, and average pore diameter of SWCNTs (16). However, the surface area of pore size ≤ 5 nm increases after the SWCNTs were oxidized by HNO_3 and NaClO solutions, probably because of the removal of the metal catalyst. The physical properties of SWCNTs have no significant changes after oxidation by the HCl solution.

Raman

Figure 5 shows the Raman spectra of adsorbents. The peak located between $1330-1360\ cm^{-1}$ is the so-called D band which is related to disordered

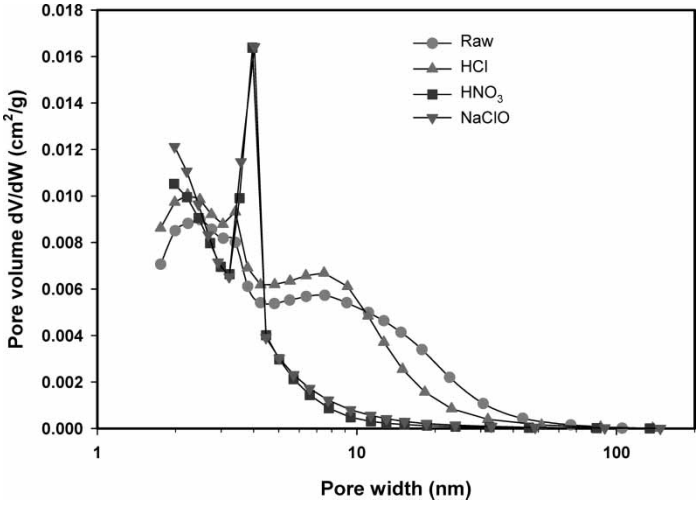

Figure 4. Pore size distributions of adsorbents.

sp^2-hybidized carbon atoms of nanotubes. The peak near 1580 cm^{-1} is the so-called G band which is related to the graphite E_{2g} symmetry of the interlayer mode. This mode reflects the structural integrity of sp^2-hybridized carbon atoms of the nanotubes. Together, these bands can be used to evaluate the extent of carbon-containing defects (17–19). The intensity ratios of D band to G band (I_D/I_G) of SWCNTs, SWCNTs(HCl), SWCNTs(HNO_3) and SWCNTs(NaClO) are 0.044, 0.038, 0.130, and 0.164, respectively. The Raman intensities of SWCNTs and SWCNTs(HCl) are higher than those of SWCNTs(HNO_3) and SWCNTs(NaClO) but the I_D/I_G ratios are lower than those of SWCNTs(HNO_3) and SWCNTs(NaClO). This indicates that the

Table 1. Physical properties of adsorbents

	<1.7 nm			1.7–100 nm				
				1.7–5.0 nm		5.0–100 nm		
Adsorbents	SA	PV	APD	SA	PV	SA	PV	APD
Raw	206	0.27	1.28	388	0.28	285	0.79	6.87
HCl	202	0.29	1.57	387	0.28	286	0.84	7.08
HNO_3	362	0.26	0.93	395	0.3	40	0.1	3.65
NaClO	365	0.26	0.71	423	0.31	54	0.15	3.9

Note: SA = Surface area (m^2/g), PV = pore volume (cm^3/g), APD = average pore diameter (nm).

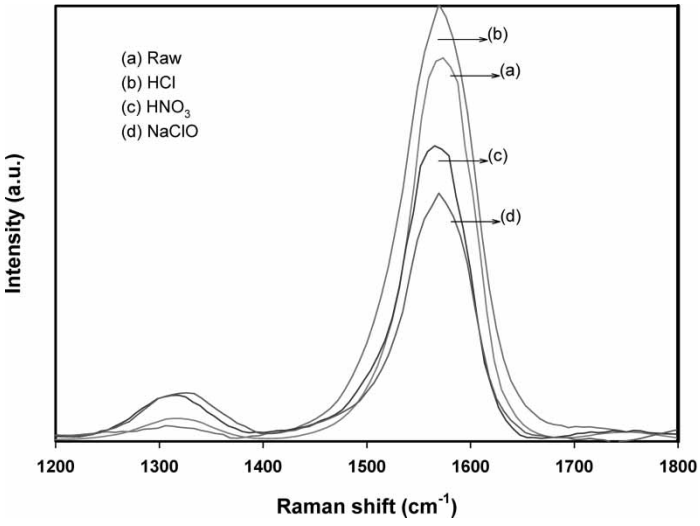

Figure 5. Raman spectra of adsorbents.

SWCNTs and SWCNTs(HCl) possess more graphitized structures and less carbon-containing defects, which are consistent with the TEM observations.

FTIR

Figure 6 exhibits the IR spectra of the adsorbents. The intense and broad bands for the SWCNTs(HNO_3) and SWCNTs(NaClO) are stronger than those of SWCNTs and SWCNTs(HCl), indicating that the SWCNTs possess more surface functional groups after oxidation by HNO_3 and NaClO solutions. This could be explained by the increase in structure defects as indicated in TEM images and Raman spectra. These functional groups produced abundantly on the external and internal surface of SWCNT pores, which can provide numerous chemical sorption sites and thus increase the adsorption capacity for the IPA vapor. The peak at 3430 cm^{-1} can be assigned to -OH stretch from carboxylic groups (-COOH and -COH) (20). The peaks at 2850–2960, 1722, and 1050–1610 cm^{-1} can be related to asymmetric and symmetric C-H stretching vibrating in aliphatic, carboxylic acids and phenolic groups (O-H), aromatic ring groups and quinine (C═O) respectively (21, 22). There are also other functional groups attached on the surface of raw and oxidized SWCNTs.

Boehm Titration

The Boehm titration showed that the SWCNTs(NaClO) contain the greatest amount of surface basic site (0.648 mmol/g), followed by the

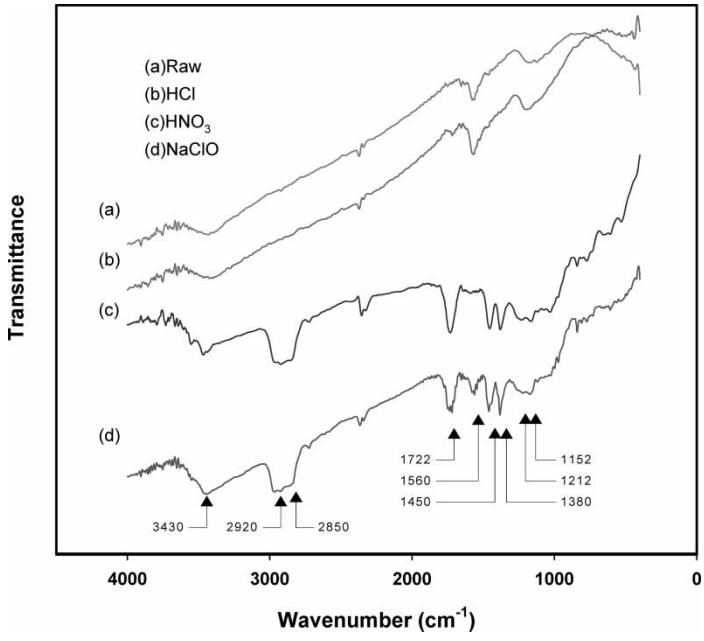

Figure 6. Fourier transform infrared spectra of adsorbents.

SWCNTs(HNO_3) (0.428 mmol/g), the SWCNTs (0.391 mmol/g) and then the SWCNTs(HCl) (0.370 mmol/g). The surface basic sites have intermediate affinity for adsorption of IPA from air streams.

TGA

Figure 7 reveals the TG analyses of raw and oxidized SWCNTs. It is evident that the SWCNTs and SWCNTs(HCl) are considerably stable and show a little weight loss close to 3% below 500°C, which could be attributed to better graphite structures. A significant weight loss begins at 500–550°C and ends at ~700°C, in which 3.5 and 3.6% remaining weight was found for the SWCNTs and SWCNTs(HCl), respectively. The SWCNTs(HNO_3) and SWCNTs(NaClO) have a broader temperature range for weight loss and exhibit three main weight loss regions. The first weight loss region can be attributed to the loss of various kinds of functional groups on the surface of SWCNTs. The rapid weight loss region can be assigned to the decomposition of SWCNTs. The third region only shows very little weight loss, close to 2%, in which 5.5 and 9.5% remaining weight was observed for the SWCNTs(HNO_3) and SWCNTs(NaClO), respectively. The carbon content in the SWCNTs decreased from 96.5 to 96.4, 94.5 and 90.5% after oxidation by HCl, HNO_3 and NaClO solutions.

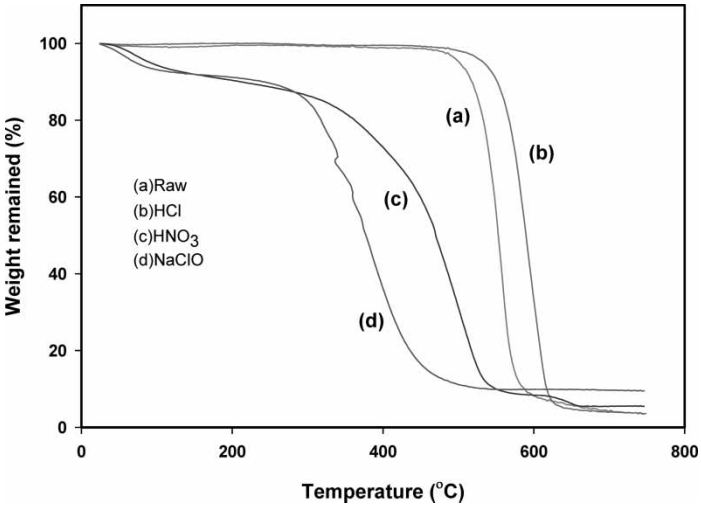

Figure 7. Thermogravimetric analyses of adsorbents.

Adsorption Isotherms

The q_e are correlated with the isotherm models of Langmuir Eqn (4), Freundlich Eqn (5) and BET Eqn (6):

$$q_e = \frac{q_m b C_e}{1 + bC_e} \tag{4}$$

$$q_e = K_F C_e^{1/n} \tag{5}$$

$$q_e = \frac{q_m K_B C_e}{(1 - C_e/C_s)(C_s - C_e + K_B C_e)} \tag{6}$$

where C_e and C_s are the equilibrium and saturation IPA concentrations, respectively, (mg/l); q_m is the maximum IPA adsorption capacity (mg/g); b is the Langmuir adsorption constant (ppmv^{-1}); K_F and n are the Freundlich constants; and K_B is the BET constant. The constants of these isotherm models were obtained from fitting the isotherm model to the q_e and C_e, and are given in Table 2. As can be observed, the correlation coefficients of Langmuir and BET models are very close and higher than those of Freundlich model. The q_m and K_F, which represent the IPA adsorption capacity, are the greatest for the SWCNTs(NaClO), followed by the SWCNTs(HNO_3), SWCNTs and then the SWCNTs(HCl). The constant K_B, which is related to the energy of interaction between the IPA vapor and the adsorbent surface, is the most for the SWCNTs(NaClO), followed by the SWCNTs(HNO_3), SWCNTs(HCl), and then the SWCNTs. The SWCNTs(NaClO) show the best preference of IPA removal.

Table 2. Constants of isotherm models

Isotherm models	Raw	HCl	HNO_3	NaClO
Langmuir				
q_m	63.48	54.34	72.99	103.56
b	0.0040	0.0041	0.0104	0.0086
R^2	0.987	0.992	0.993	0.986
Freundlich				
K_F	1.10	1.07	4.99	7.15
$1/n$	0.593	0.571	0.413	0.388
R^2	0.967	0.962	0.985	0.949
BET				
q_m	56.35	47.04	77.29	97.84
K_B	206.35	227.08	372.06	410.22
R^2	0.992	0.994	0.986	0.996

Note: q_m = mg/g; b = $ppmv^{-1}$; K_F = (mg/g) $(ppmv)^n$; n, K_B and R = dimensionless.

Langmuir isotherms of IPA onto adsorbents are shown in Fig. 8. The curves of SWCNTs(HNO_3) and SWCNTs(NaClO) are much higher than those of SWCNTs and SWCNTs(HCl). The q_m of SWCNTs, SWCNTs(HCl), SWCNTs(HNO_3) and SWCNTs(NaClO) are 63.48, 54.34, 72.99, and 103.56 mg/g, respectively.

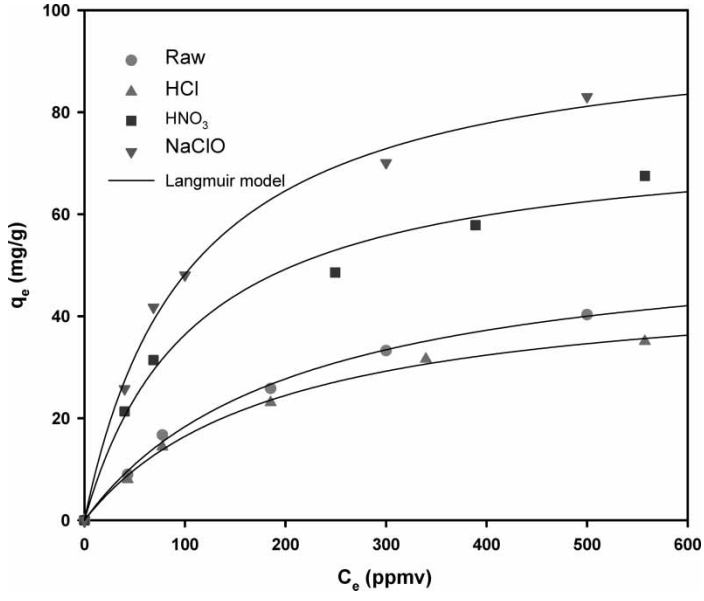

Figure 8. Adsorption isotherms of IPA onto adsorbents.

Physisorption/Chemisorption Processes

Physisorption occurs due to van der Waals' forces between the adsorbate molecules and the adsorbents while chemisorption takes place due to chemical interactions between the adsorbate molecules and the surface functional groups of adsorbents. A distinction between these two processes is very useful in understanding the factors that influence the adsorption rate. Figure 9 shows the q_{ec} and q_{ep} of adsorbents with a C_{in} of 500 ppmv. It is evident that the q_{ep} increased from 29.5 mg/g to 42.7 and 39.5 mg/g and the q_{ec} increased from 10.8 mg/g to 26.8 and 43.5 mg/g after the SWCNTs were oxidized by HNO_3 and NaClO solutions, respectively. The increase in q_{ep} could be attributed to the decrease in pore size of SWCNTs, which are closer to the size of IPA molecules (3), consequently increasing the physical forces of attachment between SWCNTs and IPA vapor. Moreover, the increase in the surface area of micropores may also enhance the physical forces of attachment. The increase in q_{ec} could be due to the increase in surface basic sites. However, both q_{ep} and q_{ec} decreased after the SWCNTs were oxidized by HCl solution, probably because of the increase in the size of micropores and the decrease in surface basic sites.

Figure 10 shows the effect of inlet IPA concentration (C_{in}) on the q_{ec} and q_{ep} of adsorbents. It is apparent that both q_{ec} and q_{ep} increased with C_{in}, This could be explained by the fact that the diffusion driving force would be greater with a higher C_{in}, which causes a faster diffusion rate of IPA vapor across the external boundary layer and within the pores of SWCNTs, consequently resulting in adsorption of more IPA vapors. The q_{ep} is much greater than the q_{ec} for the SWCNTs across the C_{in} range tested and for the

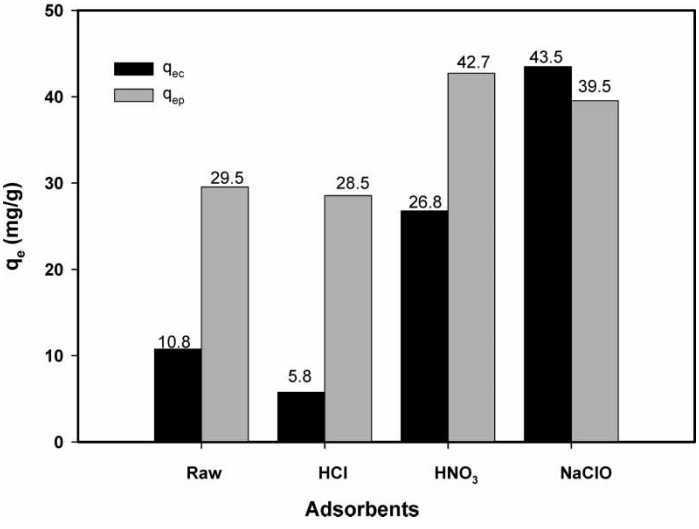

Figure 9. Physisorption and chemisorption capacities of IPA onto adsorbents.

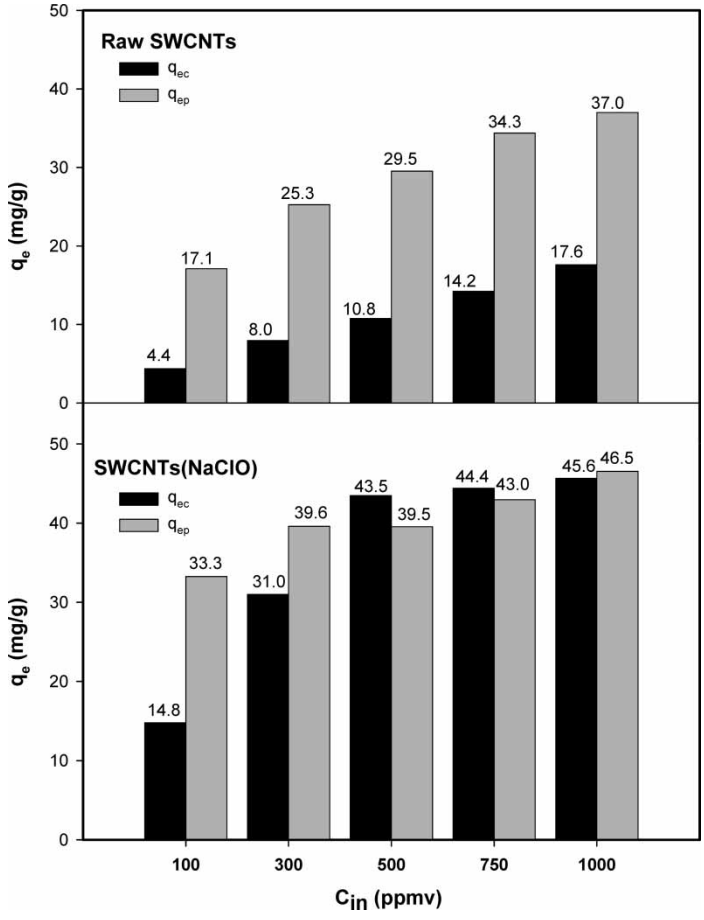

Figure 10. Physisorption and chemisorption capacities of IPA onto raw and NaClO oxidized SWCNTs under various inlet concentrations.

SWCNTs(NaClO) with a relatively low C_{in} ($\leq$300 ppmv). However, the q_{ep} is nearly the same as the q_{ec} for the SWCNTs(NaClO) with $C_{in} \geq 500$ ppmv. These results indicate that the adsorption mechanism of IPA vapor appears mainly attributable to physical force for the SWCNTs and SWCNTs(NaClO) with a relatively low C_{in} but appears attributable to both physical and chemical forces for the SWCNTs(NaClO) with a relatively high C_{in}.

CONCLUSIONS

The raw and HCl, HNO_3, NaClO oxidized SWCNTs were selected as adsorbents to study their characterizations and adsorption properties of IPA

from air streams. The physicochemical properties of SWCNTs were greatly improved after oxidation by HNO_3 and NaClO solutions including the decrease in pore size and the increase in defective structures, surface areas of micropores, surface functional groups, and surface basic sites. These modifications made SWCNTs that adsorb more IPA from air streams. The SWCNTs(NaClO) have the best performance of IPA removal, followed by the SWCNTs(HNO_3), the SWCNTs, and then the SWCNTs(HCl), suggesting that the SWCNTs(NaClO) are promising IPA adsorbents. The adsorption mechanism of IPA vapor appears mainly attributable to physical force for the SWCNTs and SWCNTs(NaClO) with a relatively low C_{in} but appears attributable to both physical and chemical forces for the SWCNTs(NaClO) with a relatively high C_{in}.

ACKNOWLEDGEMENTS

Support from the National Science Council, Taiwan, under contract no. NSC 95-2211-E-005-058-MY2 is gratefully acknowledged.

REFERENCES

1. Smart, S.K., Cassady, A.I., Lu, G.Q., and Martin, D.J. (2006) The biocompatibility of carbon nanotubes. *Carbon*, 44: 1034–1047.
2. Long, Q.R. and Yang, R.T. (2001) Carbon nanotubes as superior sorbent for dioxin removal. *J. Am. Chem. Soc.*, 123: 2058–2059.
3. Agnihotri, S., Rood, M.J., and Rostam-Abadi, M. (2005) Adsorption equilibrium of organic vapors on single-walled carbon nanotubes. *Carbon*, 43: 2379–2388.
4. Li, Y.H., Wang, S., Wei, J., Zhang, X., Xu, C., Luan, Z., Wu, D., and Wei, B. (2002) Lead adsorption on carbon nanotubes. *Chem. Phys. Lett.*, 357: 263–266.
5. Li, Y.H., Wang, S., Luan, Z., Ding, J., Xu, C., and Wu, D. (2003) Adsorption of cadmium (II) from aqueous solution by surface oxidized carbon nanotubes. *Carbon*, 41: 1057–1062.
6. Li, Y.H., Wang, S., Wei, J., Zhang, X., Xu, C., Luan, Z., and Wu, D. (2003) Adsorption of fluoride from water by aligned carbon nanotubes. *Mater. Res. Bull.*, 38: 469–476.
7. Peng, X., Li, Y., Luan, Z., Di, Z., Wang, H., Tian, B., and Jia, Z. (2003) Adsorption of 1,2-dichlorobenzene from water to carbon nanotubes. *Chem. Phys. Lett.*, 376: 154–158.
8. Lu, C., Chung, Y.L., and Chang, K.F. (2005) Adsorption of trihalomethanes from water with carbon nanotubes. *Wat. Res.*, 39: 1183–1189.
9. Lu, C. and Chiu, H. (2006) Adsorption of zinc (II) from water with purified carbon nanotubes. *Chem. Eng. Sci.*, 61: 1134–1141.
10. Lu, C. and Liu, C. (2006) Removal of nickel (II) from aqueous solution by carbon nanotubes. *J. Chem. Technol. Biotechnol.*, 81: 1932–1940.
11. Purdom, P.W. (1980) *Environmental Health, 2nd Edn*; Academic Press: New York.

12. Yin, C.Y., Aroua, M.K., and Daud, W.M.A.W. (2007) Review of modifications of activated carbon for enhancing contaminant uptakes from aqueous solutions. *Sep. Purif. Technol.*, 52: 403–415.
13. Boehm, H.P. (1994) Some aspects of the surface chemistry of carbon blacks and other carbons. *Carbon*, 32: 759–769.
14. Gregg, S.J. and Sing, K.S.W. (1982) *Adsorption, Surface Area and Porosity*; Academic Press: New York.
15. Hsieh, C.T. and Chou, Y.W. (2006) Fabrication and vapor-phase adsorption characterization of acetone and *n*-hexane onto carbon nanofibers. *Sep. Sci. Technol.*, 41: 3155–3168.
16. Chingombe, P., Saha, B., and Wakeman, R.J. (2005) Surface modification and characterization of a coal-based activated carbon. *Carbon*, 43: 3132–3143.
17. Tsai, C.L. and Chen, C.F. (2003) Characterization of bias-controlled carbon nanotubes. *Diamond Relat. Mater.*, 12: 1615–1620.
18. Dresselhaus, M.S., Dresselhaus, G., Jorio, A., Souza Filho, A.G., and Saito, R. (2002) Raman spectroscopy on isolated single wall carbon nanotubes. *Carbon*, 40: 2043–2061.
19. Ko, C.J., Lee, C.Y., Ko, F.H., Chen, H.L., and Chu, T.C. (2004) Highly efficient microwave-assisted purification of mulltiwalled carbon nanotubes. *Microelectronic Eng.*, 73–74: 570–577.
20. Huang, H.Y., Yang, R.T., Chinn, D., and Munson, C.L. (2003) Amine-grafted MCM-48 and silica xerogel as superior sorbents for acid gas removal from natural gas. *Ind. Eng. Chem. Res.*, 42: 2427–2433.
21. David, W.M., Erickson, C.L., Johnston, C.T., Delfino, J.J., and Porter, J.E. (1999) Quantitative Fourier transform infrared spectroscopic investigation of humic substance functional group composition. *Chemosphere*, 38: 2913–2928.
22. Ovejero, G., Sotelo, J.L., Romero, M.D., Rodríguez, A., Ocaña, M.A., Rodríguez, G., and García, J. (2006) Multiwalled carbon nanotubes for liquid-phase oxidation. Functionalization, characterization, and catalytic activity. *Ind. Eng. Chem. Res.*, 45: 2206–2212.